Strong Equivalence of the Interleaving and Functional Distortion Metrics for Reeb Graphs

Ulrich Bauer[1], Elizabeth Munch[2], and Yusu Wang[3]

1 Department of Mathematics, Technische Universität München (TUM), Germany
mail@ulrich-bauer.org
2 Department of Mathematics & Statistics, University at Albany – SUNY, USA
emunch@albany.edu
3 Department of Computer Science and Engineering, The Ohio State University, USA
yusu@cse.ohio-state.edu

Abstract

The Reeb graph is a construction that studies a topological space through the lens of a real valued function. It has been commonly used in applications, however its use on real data means that it is desirable and increasingly necessary to have methods for comparison of Reeb graphs. Recently, several metrics on the set of Reeb graphs have been proposed. In this paper, we focus on two: the functional distortion distance and the interleaving distance. The former is based on the Gromov–Hausdorff distance, while the latter utilizes the equivalence between Reeb graphs and a particular class of cosheaves. However, both are defined by constructing a near-isomorphism between the two graphs of study. In this paper, we show that the two metrics are strongly equivalent on the space of Reeb graphs. Our result also implies the bottleneck stability for persistence diagrams in terms of the Reeb graph interleaving distance.

1998 ACM Subject Classification F.2.2 Nonnumerical Algorithms and Problems: Geometrical problems and computations

Keywords and phrases Reeb graph, interleaving distance, functional distortion distance

Digital Object Identifier 10.4230/LIPIcs.SOCG.2015.461

1 Introduction

The Reeb graph is a construction that can be used to study a topological space with a real valued function by tracking the relationships between connected components of level sets. It was originally developed in the context of Morse theory [21], and was later introduced for shape analysis by Shinagawa et al. [23]. Since then, it has attracted much attention due to its wide use for various data analysis applications, such as shape comparison [15, 11], denoising [25], and shape understanding [7, 14]; see [2] for a survey. Recently, the applications of Reeb graphs have been further broadened to summarizing high-dimensional and/or complex data, in particular, reconstructing non-linear 1-dimensional structure in data [18, 12, 4] and summarizing collections of trajectory data [3]. Its practical applications have also been facilitated by the availability of efficient algorithms for computing the Reeb graph from a piecewise-linear function defined on a simplicial complex [20, 13, 9].

In addition to the standard construction, a generalization of the Reeb graph construction, known as Mapper, [24], has proven extremely useful in the field of topological data analysis [26, 19]. A variant of Mapper for real-valued functions, called the α-Reeb graph, was used in [4] to study data sets with 1-dimensional structure.

31st International Symposium on Computational Geometry (SoCG'15).
Editors: Lars Arge and János Pach; pp. 461–475
Leibniz International Proceedings in Informatics
LIPICS Schloss Dagstuhl – Leibniz-Zentrum für Informatik, Dagstuhl Publishing, Germany

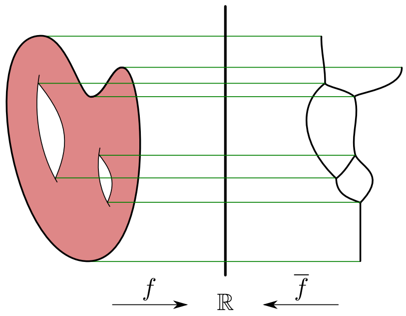

Figure 1 A simple example of the Reeb graph (right) of a space (left). Here and in all other drawn examples in this paper, the real valued function is indicated by vertical height.

Given the popularity of the Reeb graph and related constructions for practical data analysis applications, it is desirable and increasingly necessary to understand how robust (stable) these structures are in the presence of noise. Consequently, several metrics for comparing Reeb graphs have been proposed recently. These include the functional distortion distance [1], the interleaving distance [6], and the combinatorial edit distance [8]. We note that the latter is limited to Reeb graphs resulting from Morse functions defined on surfaces. In addition, Morozov et. al proposed an interleaving distance for a simpler variant of the Reeb graph, the *merge tree* [17].

In this paper, we study the relation between two recently proposed distances for general Reeb graphs: the functional distortion distance of [1] and the interleaving distance of [6]. The former is based on concepts from metric geometry, and is defined by treating both graphs as metric spaces and inspecting continuous maps between them. The latter, on the other hand, is defined using ideas of category theory, utilizing the equivalence between Reeb graphs and a particular class of cosheaves. However, in essence, both construct a near-isomorphism between the two input graphs of study. In Sections 3 and 4, we explore this connection between the two distances, and show that indeed, the functional distortion distance and the interleaving distances are strongly equivalent on the space of Reeb graphs, meaning that they are within a constant factor of each other. This immediately leads to the bottleneck stability result for the Reeb graph interleaving distance.

2 Definitions

Given a topological space $\mathbb{W}$ with a real valued function $f : \mathbb{W} \to \mathbb{R}$, we define the Reeb graph of $(\mathbb{W}, f)$ as follows. We say that two points in $\mathbb{W}$ are equivalent if they are in the same path component of a level set $f^{-1}(a)$ for $a \in \mathbb{R}$. This is denoted as $x \sim_f y$, or $x \sim y$ if the function is obvious. Then the Reeb graph is the quotient space $\mathbb{W}/\sim_f$. Note that the Reeb graph inherits a real valued function from its parent space. See Fig. 1 for an example.

2.1 Category of Reeb Graphs

For nice enough functions $f : \mathbb{W} \to \mathbb{R}$, such as Morse functions on compact manifolds or PL functions on finite simplicial complexes, the Reeb graph is, in fact, a finite graph [6]. We will tacitly make this assumption on the Reeb graph throughout the paper. Thus, we will define the category of Reeb graphs, following [6], intuitively to be finite graphs with real valued functions that are strictly monotonic on the edges. Morphisms will be given by function preserving maps between the underlying spaces as given in the following definition.

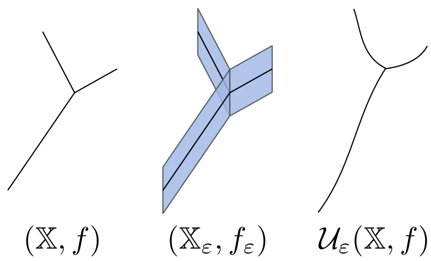

Figure 2 An example of a smoothed Reeb graph. Shown on the left is the original graph $\mathbb{X}$, with the function f given by height. The middle space is $\mathbb{X}_\varepsilon = \mathbb{X} \times [-\varepsilon, \varepsilon]$ with the function $f_\varepsilon(x,t) = f(x) + t$ still given by height. On the right is the Reeb graph of $(\mathbb{X}_\varepsilon, f_\varepsilon)$, which is the smoothed Reeb graph $\mathcal{U}_\varepsilon(\mathbb{X})$.

▶ **Definition 1.** An object of the category **Reeb** is a finite graph, seen as a topological space $\mathbb{X}$ (specifically, as a regular CW complex of dimension 1), together with a real valued function that is strictly monotonic on edges. This will equivalently be written as either $f : \mathbb{X} \to \mathbb{R}$ or $(\mathbb{X}, f)$. A morphism between $(\mathbb{X}, f)$ and $(\mathbb{Y}, g)$ is a function preserving map $\varphi : \mathbb{X} \to \mathbb{Y}$, i.e., the following diagram commutes:

$$\begin{array}{ccc} \mathbb{X} & \xrightarrow{\varphi} & \mathbb{Y} \\ & {\scriptstyle f}\searrow & \downarrow{\scriptstyle g} \\ & & \mathbb{R} \end{array}$$

Note that since we assume that the function is strictly monotonic when restricted to the edges, it is defined up to isomorphism by the values on the vertices. As an aside, notice that the quotient map sending a space with a function to its Reeb graph is an isomorphism when the space is in **Reeb**.

2.2 Interleaving Distance

Given a Reeb graph $(\mathbb{X}, f)$, let $\mathbb{X}_\varepsilon$ denote the space $\mathbb{X} \times [-\varepsilon, \varepsilon]$, and define the ε-smoothing of $(\mathbb{X}, f)$ as the Reeb graph of the function

$$\begin{array}{rccc} f_\varepsilon : & \mathbb{X}_\varepsilon & \to & \mathbb{R}, \\ & (x,t) & \mapsto & f(x) + t. \end{array}$$

That is, the ε-smoothing is the quotient space $\mathbb{X}_\varepsilon / \sim_{f_\varepsilon}$. Denote this space by $\mathcal{U}_\varepsilon(\mathbb{X}, f)$ and note that $\mathcal{U}_\varepsilon(\mathcal{U}_\varepsilon(\mathbb{X}, f)) \cong \mathcal{U}_{2\varepsilon}(\mathbb{X}, f)$ [6]. Sometimes when we are focusing on the underlying topological space and the function is obvious, we will denote this as $\mathcal{U}_\varepsilon(\mathbb{X})$. See Fig. 2 for an example.

An ε-interleaving of $(\mathbb{X}, f)$ and $(\mathbb{Y}, g)$ is a pair of function preserving maps (as in Definition 1) $\varphi : (\mathbb{X}, f) \to \mathcal{U}_\varepsilon(\mathbb{Y}, g)$ and $\psi : (\mathbb{Y}, g) \to \mathcal{U}_\varepsilon(\mathbb{X}, f)$ with the following requirements. Consider the maps

$$\begin{aligned} \iota : (\mathbb{X}, f) &\to \mathcal{U}_\varepsilon(\mathbb{X}, f), & x &\mapsto [x, 0], \\ \iota_\varepsilon : \mathcal{U}_\varepsilon(\mathbb{Y}, g) &\to \mathcal{U}_{2\varepsilon}(\mathbb{Y}, g), & [x,t] &\mapsto [x,t], \\ \varphi_\varepsilon : \mathcal{U}_\varepsilon(\mathbb{X}, f) &\to \mathcal{U}_{2\varepsilon}(\mathbb{Y}, g), & [x,t] &\mapsto [\varphi(x), t], \end{aligned}$$

where $[x,t] = q(x,t)$ is the equivalence class of (x,t) under the quotient map $q : \mathbb{X}_\varepsilon \to \mathcal{U}_\varepsilon(\mathbb{X}, f)$.

Note that the diagram

$$\begin{array}{ccc} (\mathbb{X}, f) & \xrightarrow{\iota} & \mathcal{U}_\varepsilon(\mathbb{X}, f) \\ {\scriptstyle\varphi}\downarrow & & \downarrow{\scriptstyle\varphi_\varepsilon} \\ \mathcal{U}_\varepsilon(\mathbb{Y}, g) & \xrightarrow{\iota_\varepsilon} & \mathcal{U}_{2\varepsilon}(\mathbb{Y}, g) \end{array}$$

commutes. Analogously defining maps $\iota : (\mathbb{Y}, g) \to \mathcal{U}_\varepsilon(\mathbb{Y}, g)$, $\iota_\varepsilon : \mathcal{U}_\varepsilon(\mathbb{X}, f) \to \mathcal{U}_{2\varepsilon}(\mathbb{X}, f)$, and $\psi_\varepsilon : \mathcal{U}_\varepsilon(\mathbb{Y}, g) \to \mathcal{U}_{2\varepsilon}(\mathbb{X}, f)$, we have the following definition of an ε-interleaving.

▶ **Definition 2** (ε-Interleaving)**.** The maps $\varphi : (\mathbb{X}, f) \to \mathcal{U}_\varepsilon(\mathbb{Y}, g)$ and $\psi : (\mathbb{Y}, g) \to \mathcal{U}_\varepsilon(\mathbb{X}, f)$ are an *ε-interleaving* if both of them are function preserving, and the following diagram

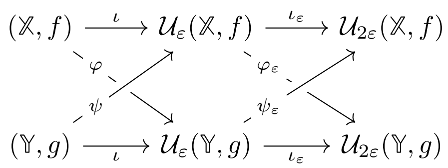

commutes.

We can use this definition of interleavings to define a distance on Reeb graphs.

▶ **Definition 3** (Interleaving Distance, [6])**.** The *interleaving distance* between two Reeb graphs $(\mathbb{X}, f)$ and $(\mathbb{Y}, g)$ is defined to be

$$d_I((\mathbb{X}, f), (\mathbb{Y}, g)) = \inf \{\varepsilon \mid \text{there exists an } \varepsilon\text{-interleaving between } (\mathbb{X}, f), (\mathbb{Y}, g)\}.$$

The definition of the interleaving distance was motivated by the cosheaf structure of Reeb graphs. It was shown in [6] that the category of Reeb graphs is equivalent to a particular class of cosheaves, which can be thought of as functors $\mathsf{F} : \mathbf{Int} \to \mathbf{Set}$ giving a set for each open interval. Specifically, given a real-valued function $f : \mathbb{X} \to \mathbb{R}$, we can construct the associated functor $\mathsf{F} = \pi_0 \circ f^{-1}$, where π_0 sends a topological space to its set of path components. This equivalence allows us to work with either the topological construction or the category theoretic one, whichever is easier or more appropriate. An excellent introduction to cellular cosheaves can be found in [5].

2.3 Functional Distortion Distance

For a given path π from u to v in $(\mathbb{X}, f) \in \mathbf{Reeb}$, we define the height of the path to be

$$\text{height}(\pi) = \max_{x \in \pi} f(x) - \min_{x \in \pi} f(x).$$

Then we define the distance

$$d_f(u, v) = \min_{\pi : u \rightsquigarrow v} \text{height}(\pi)$$

where π ranges over all paths from u to v in $\mathbb{X}$. Note that this can be equivalently defined by the minimum length of any closed interval I such that u and v are in the same path component of $f^{-1}(I)$.

The functional distortion distance between $(\mathbb{X}, f)$ and $(\mathbb{Y}, g)$ is now defined as follows:

▶ **Definition 4** (Functional Distortion Distance, [1]). Given $(\mathbb{X}, f), (\mathbb{Y}, g) \in \mathbf{Reeb}$ and maps $\Phi : \mathbb{X} \to \mathbb{Y}$ and $\Psi : \mathbb{Y} \to \mathbb{X}$, let

$$C(\Phi, \Psi) = \{(x, y) \in \mathbb{X} \times \mathbb{Y} \mid \Phi(x) = y \text{ or } x = \Psi(y)\}$$

and

$$D(\Phi, \Psi) = \sup_{\substack{(x,y),(x',y') \\ \in C(\Phi,\Psi)}} \frac{1}{2} \left| d_f(x, x') - d_g(y, y') \right|.$$

Then the *functional distortion distance* is defined to be

$$d_{FD}(f, g) = \inf_{\Phi,\Psi} \max\{D(\Phi, \Psi), \|f - g \circ \Phi\|_\infty, \|g - f \circ \Psi\|_\infty\}.$$

Note that since the maps Φ, Ψ are not required to preserve the function values, they are not necessarily Reeb graph morphisms in the sense of Definition 1.

2.4 Multivalued Maps and Continuous Selections

In order to prove our main result, we will make heavy use of the theory of multivalued maps and the notion of a selection of such a map. We briefly introduce the required definitions and a central result asserting the existence of a continuous selection.

A multivalued map (or multimap) $F : X \to Y$ is a relation $F \subseteq X \times Y$ that sends a point $x \in X$ to a nonempty set $F(x) = \{y \in Y \mid \exists x \in X : (x, y) \in F\} \subset Y$. A selection of a multimap is a map $f : X \to Y$ such that $f(x) \in F(x)$ for every $x \in X$. See [22] for an introduction to multimaps.

Note that using the axiom of choice, a selection always exists; the difficulty is in finding a continuous selection. The Michael selection theorem gives a criterion for a multimap to have a continuous selection. However, in order to state it, we will need several definitions.

▶ **Definition 5.** A family $\mathcal{S}$ of subsets of a topological space Y is equi-locally n-connected if for every $S \in \mathcal{S}$, every $y \in S$, and every neighborhood W of y, there is a neighborhood V of y such that $V \subset W$ and for every $S' \in \mathcal{S}$ such that $V \cap S' \neq \emptyset$, every continuous mapping of the m-sphere $\mathbb{S}^m$ into $S' \cap V$ is null-homotopic in $S' \cap W$ for $m \leq n$. This is denoted by $\mathcal{S} \in \mathrm{ELC}^n$.

In particular, we will be requiring the case where $\mathcal{S} \in \mathrm{ELC}^0$. A sufficient condition for this to hold is that in the above definition, V can be chosen such that for any $S' \in \mathcal{S}$, the intersection $S' \cap V$ is either empty or path connected.

▶ **Definition 6.** A multivalued map $F : X \to Y$ is lower semicontinuous (LSC) if for every open set $U \subset Y$ the set $F^{-1}(U) = \{x \in X \mid F(x) \cap U \neq \emptyset\}$ is open in X.

Finally we can state the Michael selection theorem. Since we are working with a space of covering dimension 1, we paraphrase the more general theorem here to relate it to our context.

▶ **Theorem 7** (Michael 1956[16]). *A multivalued mapping $F : X \to Y$ admits a continuous single-valued selection provided that the following conditions are satisfied:*

1. *X is a paracompact space with covering dimension* $\dim(X) \leq 1$*;*
2. *Y is a completely metrizable space;*
3. *F is an LSC mapping;*
4. *for every $x \in X$, $F(x)$ is a path connected subspace of Y; and*
5. *the family of values $\{F(x)\}_{x \in X}$ is* ELC^0*.*

3 ε-Interleaving and Functional Distortion

In order to prove the main result, Theorem 16, we will prove each inequality separately as Lemmas 8 and 15 .

3.1 The Easy Direction

▶ **Lemma 8.** *Let* $(\mathbb{X}, f), (\mathbb{Y}, g) \in \mathbf{Reeb}$*. Then*

$$d_I(f, g) \leq d_{FD}(f, g).$$

Proof. Let $\varepsilon > d_{FD}(f, g)$. By definition of the functional distortion metric, there are maps

$$\mathbb{X} \underset{\Psi}{\overset{\Phi}{\rightleftarrows}} \mathbb{Y}$$

that satisfy the requirements of Definition 4. In particular, x and $\Psi \circ \Phi(x)$ are connected by a path γ of height 2ε. This path is thus contained in the preimage $f^{-1}[f(x) - 2\varepsilon, f(x) + 2\varepsilon]$. As a consequence, the points $(x, 0)$ and $(\Psi \circ \Phi(x), f(x) - f(\Psi \circ \Phi(x)))$ are in the same path component of the level set $f_{2\varepsilon}^{-1}(f(x))$.

Define

$$\varphi : (\mathbb{X}, f) \to \mathcal{U}_\varepsilon(\mathbb{Y}, g), \qquad x \mapsto [\Phi(x), f(x) - g(\Phi(x))],$$
$$\psi : (\mathbb{Y}, g) \to \mathcal{U}_\varepsilon(\mathbb{X}, f), \qquad y \mapsto [\Psi(y), g(y) - f(\Psi(y))],$$

with the latter inducing the map

$$\psi_\varepsilon : \mathcal{U}_\varepsilon(\mathbb{Y}, g) \to \mathcal{U}_{2\varepsilon}(\mathbb{X}, f), \qquad [y, t] \mapsto [\Psi(y), g(y) - f(\Psi(y)) + t]$$

appearing in the definition of an interleaving. A visual representation of the map φ is given in Figure 3. We then have

$$\begin{aligned}
\psi_\varepsilon \circ \varphi(x) &= \psi_\varepsilon[\Phi(x), f(x) - g(\Phi(x))] \\
&= [\Psi \circ \Phi(x), g \circ \Phi(x) - f(\Psi \circ \Phi(x)) + f(x) - g(\Phi(x))] \\
&= [\Psi \circ \Phi(x), f(x) - f(\Psi \circ \Phi(x))] \\
&= [x, 0] = \iota_\varepsilon \circ \iota(x).
\end{aligned}$$

By an analogous argument, we also have $\varphi_\varepsilon \circ \psi(y) = [y, 0] = \iota_\varepsilon \circ \iota(y)$, and hence φ and ψ are an ε-interleaving. Since the above holds for any $\varepsilon > d_{FD}(f, g)$, the claim is now immediate. ◀

3.2 The Hard Direction

In order to show $d_{FD}((\mathbb{X}, f), (\mathbb{Y}, g)) \leq 3d_I((\mathbb{X}, f), (\mathbb{Y}, g))$, we need to start with an ε-interleaving, $\varphi : (\mathbb{X}, f) \to \mathcal{U}_\varepsilon(\mathbb{Y}, g)$ and $\psi : (\mathbb{Y}, g) \to \mathcal{U}_\varepsilon(\mathbb{X}, f)$, and construct a pair of maps satisfying the requirements of the functional distortion distance. To do this, note that the map φ induces a multimap $\overline{\varphi} : \mathbb{X} \to \mathbb{Y}_\varepsilon$, which sends a point x to the entire equivalence class of $\varphi(x)$, thought of as a subset of $\mathbb{Y}_\varepsilon$. Concretely, letting $q : \mathbb{Y}_\varepsilon \to \mathcal{U}_\varepsilon(\mathbb{Y})$ denote the Reeb graph quotient map, we have $\overline{\varphi} = q^{-1} \circ \varphi$.

This multimap, however, does not always have a continuous selection (see Figure 4 for a counterexample), so we will introduce a parameter δ to slightly enlarge the images of

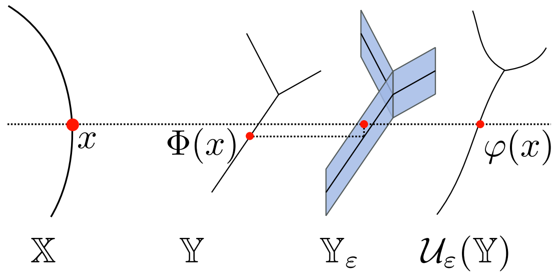

Figure 3 The definition of the map $\varphi : (\mathbb{X}, f) \to \mathcal{U}_\varepsilon(\mathbb{Y}, g)$ as given in the proof of Lemma 8.

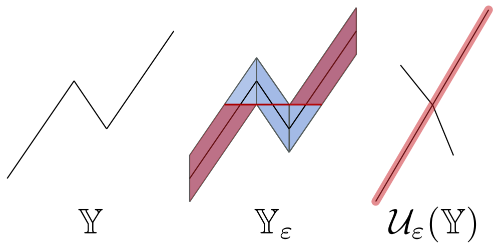

Figure 4 The map $\bar{\varphi}$ is not enough for us to have a continuous selection as seen in this counterexample. The image under $\varphi : \mathbb{X} \to \mathcal{U}_\varepsilon(\mathbb{Y})$ is the red line in the rightmost graph. However, this implies the image under $\bar{\varphi}$ is the red region in the middle space. Since with $\bar{\varphi}$, a selection may only choose one point from every level, we run into a problem in the center line since no choice of point will allow for a continuous selection.

$\bar{\varphi}$. First, note that we have metrics d_f and d_g for $\mathbb{X}$ and $\mathbb{Y}$ respectively. For an arbitrarily small $\delta > 0$, we can construct the multimap, $\bar{\varphi}_\delta : \mathbb{X} \to \mathbb{Y}_\varepsilon$ sending x to $\bar{\varphi}(B_\delta(x))$, where $B_\delta(x) = \{x' \mid d_f(x, x') < \delta\}$. Explicitly, we have

$$\bar{\varphi}_\delta(x) = \{(y', t') \in \mathbb{Y}_\varepsilon \mid x' \in \mathbb{X}, d_f(x, x') < \delta, (y', t') \in \bar{\varphi}(x')\}.$$

See Fig. 5 for an example. For technical reasons, we will assume that $\delta < L/4$, where L is the minimum height of any edge in $\mathcal{U}_\varepsilon(\mathbb{Y})$.

In order to assert the existence of a continuous selection, we now show that the multimap $\bar{\varphi}_\delta : \mathbb{X} \to \mathbb{Y}_\varepsilon$ satisfies the assumptions of Theorem 7:

1. Since $\mathbb{X}$ is a finite CW complex, it is compact and thus trivially paracompact. In addition, because it is a graph, it has covering dimension 1.
2. Since $\mathbb{Y}$ is a finite CW complex, it is completely metrizable. Therefore, $\mathbb{Y}_\varepsilon$ is also completely metrizable, being the product of two completely metrizable spaces.
3. To show that $\bar{\varphi}_\delta$ is LSC, let $U \subset \mathbb{Y}_\varepsilon$ be open. We will show that any $x \in \bar{\varphi}_\delta^{-1}(U)$ has an open neighborhood in $\bar{\varphi}_\delta^{-1}(U)$, implying that $\bar{\varphi}_\delta^{-1}(U)$ is open. Expanding the definition of $x \in \bar{\varphi}_\delta^{-1}(U)$, there is an x' with $d_f(x, x') < \delta$ such that $\bar{\varphi}(x') \cap U \neq \emptyset$. Let $r = \delta - d_f(x, x')$. We now want to show that $B_r(x) \subseteq \bar{\varphi}_\delta^{-1}(U)$. Let $x'' \in B_r(x)$. We know that $x' \in B_\delta(x'')$ since
$$d_f(x', x'') \le d_f(x', x) + d_f(x, x'') < (\delta - r) + r = \delta.$$
Since $\bar{\varphi}(x') \cap U \neq \emptyset$ and $x' \in B_\delta(x'')$, we must have $\bar{\varphi}_\delta(x'') \cap U = \bar{\varphi}(B_\delta(x'')) \cap U \neq \emptyset$ and hence $x'' \in \bar{\varphi}_\delta^{-1}(U)$.
4. Let $q : \mathbb{Y}_\varepsilon \to \mathcal{U}_\varepsilon(\mathbb{Y})$ be the quotient map. Then $q \circ \bar{\varphi}_\delta(x) = \varphi(B_\delta(x))$ is the image of a path component under a continuous map and is therefore path connected. Since $\varphi(x) \subset \mathcal{U}_\varepsilon(\mathbb{Y})$

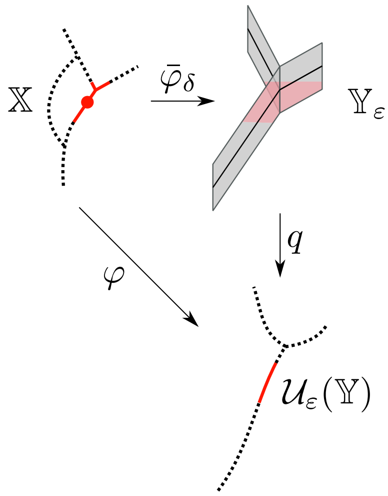

Figure 5 An example for determining the map $\bar{\varphi}_\delta$. Given the red point $x \in \mathbb{X}$, the red solid region in $\mathbb{X}$ is $B_\delta(x)$. Then we can look at $\varphi(B_\delta(x))$, the red region in $\mathcal{U}_\varepsilon(\mathbb{Y})$. The set $\bar{\varphi}_\delta(x)$ in $\mathbb{Y}_\varepsilon$ consists of the points which map into $\varphi(B_\delta(x))$ in $\mathcal{U}_\varepsilon(\mathbb{Y})$ under the quotient map q.

is by definition the image of a path component of $\mathbb{X}$, it is also path connected. So $\bar{\varphi}_\delta(x)$ can be thought of as a fibration with base space $\varphi(B_\delta(x))$ and fibers $\bar{\varphi}(x')$, for $x' \in B_\delta(x)$. Since the fibers are path connected by definition of q, and the base is path connected, the total space is path connected.

5. As checking this property is by far the most complicated, we prove it in Lemma 9.

▶ **Lemma 9.** *The family of values* $\{\bar{\varphi}_\delta(x)\}_{x\in\mathbb{X}}$ *is* ELC^0.

Proof. Fix $x \in \mathbb{X}$. Given an arbitrary $(y,t) \in \bar{\varphi}_\delta(x) \subset \mathbb{Y}_\varepsilon$ and a neighborhood W of (y,t), let $0 < r \leq \delta$ be such that $V = B_r(y,t)$ is contained in W. Here $B_r(y,t)$ denotes the open ball of radius r around (y,t) in $\mathbb{Y}_\varepsilon$ using the metric

$$d_{\mathbb{Y}_\varepsilon}((y,t),(y',t')) = d_g(y,y') + |t-t'|.$$

It suffices to show that for any $\tilde{x}$ such that $\bar{\varphi}_\delta(\tilde{x}) \cap V \neq \emptyset$, the set $\bar{\varphi}_\delta(\tilde{x}) \cap V$ is path connected. For brevity, let $U = \bar{\varphi}_\delta(\tilde{x})$. Let (y_1,t_1) and (y_2,t_2) be in the intersection $U \cap V$ and, seeking a contradiction, assume that they are in different path components of $U \cap V$. Since U is path connected, there is a path γ_1 from (y_1,t_1) to (y_2,t_2) with $\mathrm{Im}\ \gamma_1 \subset U = \bar{\varphi}_\delta(\tilde{x})$. Thus for every $s \in [0,1]$ there is an $x_s \in B_\delta(\tilde{x})$ such that $\gamma_1(s) \in \bar{\varphi}(x_s)$. The map $\bar{\varphi}$ is function preserving, so $g_\varepsilon(\gamma_1(s)) = f(x_s)$. Moreover, as $x_s \in B_\delta(\tilde{x})$, we have $|f(\tilde{x}) - g_\varepsilon(\gamma_1(s))| < \delta$ and thus $\mathrm{height}(\gamma_1) < 2\delta$. On the other hand, V is path connected and so there is a path γ_2 from (y_2,t_2) to (y_1,t_1) that stays completely inside of $V = B_r(y,t)$, and thus $\mathrm{height}(\gamma_2) < 2r$.

We can now consider the paths $q \circ \gamma_1$ and $q \circ \gamma_2$ in $\mathcal{U}_\varepsilon(\mathbb{Y})$. As the endpoints of γ_2 are in different path components of $U \cap V$ and at the same time $\mathrm{Im}\ \gamma_2 \subset V$, there must be a point $v \in \mathrm{Im}\ \gamma_2$ that is not in U.

We want to show that $q(v) \notin q(\mathrm{Im}\ \gamma_1) \subset q(U)$. By definition, $\bar{\varphi}$ is the map such that $q \circ \bar{\varphi}(z) = \varphi(z)$ for any $z \in \mathbb{X}$. Thus

$$q(U) = q \circ \bar{\varphi}_\delta(\tilde{x}) = q \circ \bar{\varphi}(B_\delta(\tilde{x})) = \varphi(B_\delta(\tilde{x})).$$

Again seeking a contradiction, assume $q(v) \in q(U) = \varphi(B_\delta(\tilde{x}))$. Then there is an $x_v \in B_\delta(\tilde{x})$ such that $\varphi(x_v) = q(v)$. But this implies that $v \in \bar{\varphi}(x_v)$ and thus $v \in \bar{\varphi}_\delta(\tilde{x}) = U$, contradicting our assumption that $v \notin U$. We conclude that $q(v) \notin q(U)$; in particular, $q(v) \notin q(\operatorname{Im} \gamma_1)$.

This implies that the loop $q(\gamma_1 \bullet \gamma_2)$ is not nullhomotopic in $\mathcal{U}_\varepsilon(\mathbb{Y})$, where $\gamma_1 \bullet \gamma_2$ denotes the concatenation of the two paths. However, since we assumed that $r \leq \delta < L/4$, where L is the minimum height of any edge in $\mathcal{U}_\varepsilon(\mathbb{Y})$, we have

$$\begin{aligned} \operatorname{height}(q(\gamma_1 \bullet \gamma_2)) &= \operatorname{height}(\gamma_1 \bullet \gamma_2) \\ &\leq \operatorname{height}(\gamma_1) + \operatorname{height}(\gamma_2) \\ &< 2\delta + 2r \leq 4\delta < L, \end{aligned}$$

and therefore must be nullhomotopic in $\mathcal{U}_\varepsilon(\mathbb{Y})$. Thus, the original assumption that $\bar{\varphi}_\delta(\tilde{x}) \cap V$ is not path connected must be false. ◀

Thus, since $\bar{\varphi}$ satisfies the requirements for Theorem 7, there exists a continuous selection of $\bar{\varphi}_\delta$, that is, a map $\widetilde{\varphi}_\delta : \mathbb{X} \to \mathbb{Y}_\varepsilon$ satisfying $\widetilde{\varphi}_\delta(x) \in \bar{\varphi}(B_\delta(x))$ for all $x \in \mathbb{X}$. Likewise, there exists a continuous selection $\widetilde{\psi}_\delta : \mathbb{Y} \to \mathbb{X}_\varepsilon$ for $\bar{\psi}_\delta$. Note however that the functional distortion distance requires a pair of maps $\mathbb{X} \to \mathbb{Y}$ and $\mathbb{Y} \to \mathbb{X}$. To get there, let p_1 be either the map $\mathbb{X}_\varepsilon \to \mathbb{X}$ or $\mathbb{Y}_\varepsilon \to \mathbb{Y}$, defined by projection onto the first factor. We define our maps for the functional distortion distance to be $\Phi = p_1 \circ \widetilde{\varphi}_\delta : \mathbb{X} \to \mathbb{Y}$ and $\Psi = p_1 \circ \widetilde{\psi}_\delta : \mathbb{Y} \to \mathbb{X}$. Note that Φ and Ψ depend on the choice of δ. The remainder of this section is devoted to showing that this pair of maps induces a functional distortion of at most $3(\varepsilon + \delta)$, establishing the upper bound on the functional distortion distance.

Bounding the functional distortion

In order to prove the main result of this section, we need to establish some notation and technical lemmas. Recall that $\iota : \mathbb{X} \to \mathcal{U}_\varepsilon(\mathbb{X}, f)$ is the map that sends x to $[x, 0] = q(x, 0)$. Moreover, let $\kappa = p_1 \circ q^{-1}$. Note that both ι^{-1} and κ are multimaps, and $\iota^{-1} \subseteq \kappa$ as relations of $\mathbb{X} \times \mathcal{U}_\varepsilon(\mathbb{X}, f)$. Similarly, define $\iota_\varepsilon : \mathcal{U}_\varepsilon(\mathbb{X}, f) \to \mathcal{U}_{2\varepsilon}(\mathbb{X}, f)$ and $\kappa_\varepsilon = p_1 q_\varepsilon^{-1}$, where $q_\varepsilon : \mathcal{U}_\varepsilon(\mathbb{X}, f) \times [-\varepsilon, \varepsilon] \to \mathcal{U}_{2\varepsilon}(\mathbb{X}, f)$ is the quotient map. We have analogous maps for $(\mathbb{Y}, g)$ in place of $(\mathbb{X}, f)$, for which we use the same identifiers while ensuring that their domains will always be clear from the context. These maps are summarized in the following diagram. Note that not all parts of the diagram commute.

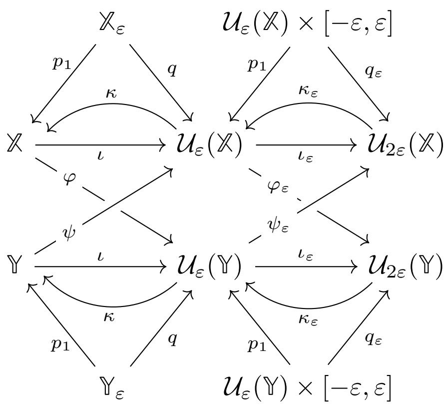

For $t \in \mathbb{R}$ and $s \geq 0$, let

$$I_s(t) := \{r \in \mathbb{R} \mid |r - t| \leq s\}$$

denote the thickening of t by s. Given any point $x \in \mathbb{X}$, we define

$$R_r(x) := \{x' \in \mathbb{X} \mid \exists \text{ path } \pi : x \rightsquigarrow x' \text{ such that } f(\text{Im } \pi) \subseteq I_r(f(x))\}.$$

That is, $R_r(x)$ is the path component of x in $f^{-1}(I_r(f(x)))$. For a subset $U \subseteq \mathbb{X}$, we define $R_r(U) := \cup_{x \in U} R_r(x)$. We can define R_r similarly for $\mathbb{Y}$, $\mathcal{U}_\varepsilon(\mathbb{X})$, or $\mathcal{U}_\varepsilon(\mathbb{Y})$. The following simple observations will be useful later; we omit the easy proof.

▶ **Lemma 10.** *(i)* $B_r(x) \subseteq R_r(x) \subseteq B_{2r}(x)$. *(ii)* $R_r(R_s(x)) \subseteq R_{r+s}(x)$.

We will now present several technical lemmas that establish how far the above diagram is from commuting.

▶ **Lemma 11.** $\kappa \circ R_r \circ \iota \subseteq R_{r+\varepsilon}$.

Proof. iven $x \in \mathbb{X}$, let $[\tilde{x}, \tilde{t}] \in R_r(\iota(x))$. We want to show that there exists a path $\pi : x \rightsquigarrow \tilde{x}$ such that $f(\text{Im } \pi) \subseteq I_{r+\varepsilon}(f(x))$. An analogous argument also holds for $y \in \mathbb{Y}$.

Since $f_\varepsilon(\iota(x)) = f(x)$ and $[\tilde{x}, \tilde{t}] \in R_r(\iota(x))$, there is a path γ from $\iota(x) = [x, 0]$ to $[\tilde{x}, \tilde{t}]$ in $\mathcal{U}_\varepsilon(\mathbb{X})$ satisfying $f_\varepsilon(\text{Im } \gamma) \subseteq I_r(f(x))$. Because the image of γ is path connected and q induces an isomorphism on path components, the subspace $q^{-1}(\text{Im } \gamma) \subset \mathbb{X}_\varepsilon$ is path connected as well. In particular, $(x, 0)$ and $(\tilde{x}, \tilde{t})$ are in this set, so there is a path ζ between them. As $\text{Im } \zeta \subseteq q^{-1}(\text{Im } \gamma)$, we have that $f_\varepsilon(\text{Im } \zeta) \subseteq f_\varepsilon(q^{-1}(\text{Im } \gamma)) = f_\varepsilon(\text{Im } \gamma) \subseteq I_r(f(x))$.

Finally, consider the path $\pi = p_1 \circ \zeta$ in $\mathbb{X}$ from x to $\tilde{x}$. Since the projection p_1 changes the function value by at most ε, we have that $f(\text{Im } \pi) \subseteq I_{r+\varepsilon}(f(x))$, and thus $\tilde{x} \in R_{r+\varepsilon}(x)$. ◀

Note that the previous lemma can also be stated using ι_ε, so we have $\kappa_\varepsilon \circ R_r \circ \iota_\varepsilon \subseteq R_{r+\varepsilon}$. Since this lemma holds for $r = 0$ as well, this also implies that $\kappa \circ \iota \subseteq R_\varepsilon$.

▶ **Lemma 12.** $\psi \circ \kappa \subseteq \kappa_\varepsilon \circ \psi_\varepsilon$.

Proof. Let $y_\varepsilon = [y, s] \in \mathcal{U}_\varepsilon(\mathbb{Y})$. Note that $y \in \kappa[y, s]$ and thus $\psi(y) \in \psi \circ \kappa[y, s]$. Since every element of $\psi \circ \kappa(y_\varepsilon)$ can be represented in this form, it suffices to show that $\psi(y) \in \kappa_\varepsilon \circ \psi_\varepsilon(y_\varepsilon)$ as well. To see this, note that by definition of ψ_ε we have $\psi_\varepsilon[y, s] = [\psi(y), s]$. Moreover, we have $\psi(y) \in \kappa_\varepsilon[\psi(y), s]$, so the claim follows. ◀

▶ **Lemma 13.** $\Psi \circ \Phi \in R_{2\varepsilon+2\delta}$.

Proof. By definition of Φ and Ψ, for any $x \in \mathbb{X}$ we have

$$\begin{aligned}\Phi(x) &= p_1 \circ \widetilde{\varphi}_\delta(x)\\ &\in p_1 \circ \overline{\varphi}(B_\delta(x))\\ &= p_1 \circ q^{-1} \circ \varphi(B_\delta(x))\\ &= \kappa \circ \varphi \circ B_\delta(x),\end{aligned}$$

and similarly for any $y \in \mathbb{Y}$ we have

$$\Psi(y) \in \kappa \circ \psi \circ B_\delta(y).$$

The composition yields

$$\Psi \circ \Phi(x) \in \kappa \circ \psi \circ B_\delta \circ \kappa \circ \varphi \circ B_\delta(x).$$

Since ψ preserves function values, a path γ in $\mathbb{Y}$ is sent to a path $\psi \circ \gamma$ of the same height in $\mathcal{U}_\varepsilon(\mathbb{X})$. Thus, for any $r \geq 0$, we have $\psi \circ B_r \subseteq B_r \circ \psi$, and so we obtain:

$$\begin{aligned}
\Psi \circ \Phi(x) &\in \kappa \circ \psi \circ B_\delta \circ \kappa \circ \varphi \circ B_\delta(x) \\
&\subseteq \kappa \circ (B_\delta \circ \psi) \circ \kappa \circ \varphi \circ B_\delta(x) && \text{since } \psi \circ B_r \subseteq B_r \circ \psi, \\
&\subseteq \kappa \circ B_\delta \circ (\kappa_\varepsilon \circ \psi_\varepsilon) \circ \varphi \circ B_\delta(x) && \text{since } \psi \circ \kappa \subseteq \kappa_\varepsilon \circ \psi_\varepsilon \text{ by Lemma 12}, \\
&\subseteq \kappa \circ B_\delta \circ \kappa_\varepsilon \circ (\iota_\varepsilon \circ \iota) \circ B_\delta(x) && \text{by the definition of an interleaving}, \\
&\subseteq \kappa \circ B_\delta \circ (R_\varepsilon) \circ \iota \circ B_\delta(x) && \text{since } \kappa_\varepsilon \circ \iota_\varepsilon \subseteq R_\varepsilon \text{ by Lemma 11}, \\
&\subseteq \kappa \circ (R_{\delta+\varepsilon}) \circ \iota \circ B_\delta(x) && \text{since } B_\delta \circ R_\varepsilon \subseteq R_{\delta+\varepsilon} \text{ by Lemma 10}, \\
&\subseteq (R_{\delta+2\varepsilon}) \circ B_\delta(x) && \text{since } \kappa \circ R_{\delta+\varepsilon} \circ \iota \subseteq R_{\delta+2\varepsilon} \text{ by Lemma 11}, \\
&\subseteq R_{2\delta+2\varepsilon}(x) && \text{since } R_{2\varepsilon} \circ B_\delta \subseteq R_{\delta+2\varepsilon} \text{ by Lemma 10}.
\end{aligned}$$ ◀

▶ **Lemma 14.** *(i)* $\|f - g \circ \Phi\|_\infty \leq \varepsilon + \delta$. *(ii)* $\|g - f \circ \Psi\|_\infty \leq \varepsilon + \delta$.

Proof. For any $x \in \mathbb{X}$, the image $\Phi(x)$ is a point in $\mathbb{Y}$ such that there is a $\tilde{x} \in \mathbb{X}$ with $d_f(x, \tilde{x}) < \delta$ and a $t \in [-\varepsilon, \varepsilon]$ with $(\Phi(x), t) \in \bar{\varphi}(\tilde{x})$. So $|f(x) - f(\tilde{x})| < \delta$ and $f(\tilde{x}) = g(\Phi(x)) + t$. Thus

$$|f(x) - g(\Phi(x))| = |f(x) - (f(\tilde{x}) - t)| = |f(x) - f(\tilde{x}) + t| \leq \delta + \varepsilon$$

and hence $\|f - g \circ \Phi\|_\infty \leq \varepsilon + \delta$. Likewise, $\|g - f \circ \Psi\|_\infty \leq \varepsilon + \delta$. ◀

Finally, we can prove the main result of this section.

▶ **Lemma 15.** *Let $f : \mathbb{X} \to \mathbb{R}$ and $g : \mathbb{Y} \to \mathbb{R}$. Then*

$$d_{FD}(f, g) \leq 3 d_I(f, g).$$

Proof. Let $\varphi : (\mathbb{X}, f) \to \mathcal{U}_\varepsilon(\mathbb{Y}, g)$ and $\psi : (\mathbb{Y}, g) \to \mathcal{U}_\varepsilon(\mathbb{X}, f)$ be an ε-interleaving, and thus $d_I(f, g) \leq \varepsilon$. As shown above, there exist continuous maps $\Phi : \mathbb{X} \to \mathbb{Y}$ and $\Psi : \mathbb{Y} \to \mathbb{X}$, constructed from selections for the multimaps $\bar{\varphi}_\delta$ and $\bar{\psi}_\delta$. Let $(x, y), (x', y') \in C(\Phi, \Psi)$. There are two cases to consider; either the pairs are of the same type (e.g., $(x, \Phi(x))$ and $(x', \Phi(x'))$), or they are different.

First assume that they are of the same type, $(x, \Phi(x))$ and $(x', \Phi(x'))$. Let γ be a minimum height path in $\mathbb{X}$ from x to x'. Then $\Phi(\gamma)$ is a path in $\mathbb{Y}$ from $\Phi(x)$ to $\Phi(x')$. Since $\|f - g \circ \Phi\|_\infty \leq \varepsilon + \delta$, the height of $\Phi(\gamma)$ exceeds the height of γ by at most $2(\varepsilon + \delta)$. So

$$\begin{aligned}
d_g(\Phi(x), \Phi(x')) &\leq \operatorname{height}(\Phi(\gamma)) \\
&\leq \operatorname{height}(\gamma) + 2(\varepsilon + \delta) \qquad (1) \\
&= d_f(x, x') + 2(\varepsilon + \delta).
\end{aligned}$$

Conversely, to get an upper bound for $d_f(x, x')$ in terms of $d_g(\Phi(x), \Phi(x'))$, let ζ be a minimum height path in $\mathbb{Y}$ between $\Phi(x)$ and $\Phi(x')$, i.e., $\operatorname{height}(\zeta) = d_g(\Phi(x), \Phi(x'))$. Note that $\Psi \circ \zeta$ is a path in $\mathbb{X}$ from $\Psi \circ \Phi(x)$ to $\Psi \circ \Phi(x')$. Since $\|g - f \circ \Psi\|_\infty \leq \varepsilon + \delta$ (Lemma 14), we have that

$$f(\Psi(\zeta)) \subseteq I_{\varepsilon+\delta}(g(\operatorname{Im} \zeta)), \qquad (2)$$

where $I_s(A) := \{r \in \mathbb{R} \mid \exists r' \in A : |r - r'| \leq s\}$ denotes the thickening of an interval $A \subseteq \mathbb{R}$ by a real number $s \geq 0$. Since $g(\Phi(x)), g(\Phi(x')) \in g(\operatorname{Im} \zeta)$, we conclude from Lemma 14 that both $f(x)$ and $f(x')$ are contained in $I_{\varepsilon+\delta}(g(\operatorname{Im} \zeta))$. Now consider the path $\widehat{\gamma} = \gamma_1 \bullet \gamma_2 \bullet \gamma_3$ in

$\mathbb{X}$ connecting x to x', where γ_1 is a mininum height path in $\mathbb{X}$ from x to $\Psi \circ \Phi(x)$, $\gamma_2 = \Psi \circ \zeta$ connects $\Psi \circ \Phi(x)$ to $\Psi \circ \Phi(x')$ as described above, and γ_3 is a minimum height path in $\mathbb{X}$ connecting $\Psi \circ \Phi(x')$ to x'. Combining Lemma 13 and (2), we obtain:

$$\begin{aligned}
f(\mathrm{Im}\ \widehat{\gamma}) &\subseteq f(\mathrm{Im}\ \gamma_1) \cup f(\mathrm{Im}\ \gamma_2) \cup f(\mathrm{Im}\ \gamma_3) \\
&\subseteq I_{2\varepsilon+2\delta}(f(x)) \cup I_{\varepsilon+\delta}(g(\mathrm{Im}\ \zeta)) \cup I_{2\varepsilon+2\delta}(f(x')) \\
&\subseteq I_{3\varepsilon+3\delta}(g(\mathrm{Im}\ \zeta)) \cup I_{\varepsilon+\delta}(g(\mathrm{Im}\ \zeta)) \cup I_{3\varepsilon+3\delta}(g(\mathrm{Im}\ \zeta)) \\
&= I_{3\varepsilon+3\delta}(g(\mathrm{Im}\ \zeta)).
\end{aligned}$$

We thus conclude

$$d_f(x, x') \leq \mathrm{height}(\widehat{\gamma}) \leq d_g(\Phi(x), \Phi(x')) + 6\varepsilon + 6\delta. \tag{3}$$

Combining the two bounds (1) and (3), we obtain

$$|d_f(x, x') - d_g(\Phi(x), \Phi(x'))| \leq 6(\varepsilon + \delta).$$

Analogously, if we are given two pairs $(\Psi(y), y), (\Psi(y'), y') \in C(\Phi, \Psi)$, we can show that

$$|d_f(\Psi(y), \Psi(y')) - d_g(y, y')| \leq 6(\varepsilon + \delta).$$

What remains to consider is the case of two pairs $(x, \Phi(x)), (\Psi(y), y) \in C(\Phi, \Psi)$. Let ξ be a minimum height path in $\mathbb{Y}$ between $\Phi(x)$ and y. By Lemma 14, $\pi_1 = \Psi \circ \xi$ is a path $\Psi(y)$ to $\Psi \circ \Phi(x)$ in $\mathbb{X}$ such that

$$f(\pi_1) \subseteq I_{\varepsilon+\delta}(g(\mathrm{Im}\ \xi)).$$

Since $g(\Phi(x)) \in g(\mathrm{Im}\ \xi)$, we also have $f(x) \in I_{\varepsilon+\delta}(g(\mathrm{Im}\ \xi))$. Now let π_2 be a minimum height path in $\mathbb{X}$ connecting x to $\Psi \circ \Phi(x)$; by Lemma 13 we have $f(\pi_2) \subseteq I_{2\varepsilon+2\delta}(f(x))$. Concatenating the two, we obtain a path $\pi = \pi_1 \bullet \pi_2$ from x to $\Psi(y)$ such that

$$\begin{aligned}
f(\mathrm{Im}\ \pi) &\subseteq f(\mathrm{Im}\ \pi_1) \cup f(\mathrm{Im}\ \pi_2) \\
&\subseteq I_{\varepsilon+\delta}(g(\mathrm{Im}\ \xi)) \cup I_{2\varepsilon+2\delta}(f(x)) \\
&\subseteq I_{\varepsilon+\delta}(g(\mathrm{Im}\ \xi)) \cup I_{3\varepsilon+3\delta}(g(\mathrm{Im}\ \xi)) \\
&= I_{3\varepsilon+3\delta}(g(\mathrm{Im}\ \xi)).
\end{aligned}$$

We conclude that

$$d_f(x, \Psi(y)) \leq d_g(\Phi(x), y) + 6\varepsilon + 6\delta.$$

Likewise, by a symmetric argument, we can show that

$$d_g(\Phi(x), y) \leq d_f(x, \Psi(y)) + 6\varepsilon + 6\delta.$$

Hence $|d_f(x, \Psi(y)) - d_g(\Phi(x), y)| \leq 6(\varepsilon + \delta)$.

Combining all of these bounds gives

$$D(\Phi, \Psi) = \sup_{\substack{(x,y),(x',y') \\ \in C(\Phi,\Psi)}} \frac{1}{2} |d_f(x, x') - d_g(y, y')| \leq 3(\varepsilon + \delta).$$

and therefore, together with Lemma 14,

$$d_{FD}(f, g) = \inf_{\Phi,\Psi} \max\{D(\Phi, \Psi), \|f - g \circ \Phi\|_\infty, \|g - f \circ \Psi\|_\infty\} \leq 3(\varepsilon + \delta).$$

Since the above holds for any $\varepsilon > d_I(f, g)$ and for any $\delta > 0$, this completes the proof. ◀

Putting together Lemmas 8 and 15, our main result is immediate.

▶ **Theorem 16.** *The functional distortion metric and the interleaving metric are strongly equivalent. That is, given any Reeb graphs* $(\mathbb{X}, f)$ *and* $(\mathbb{Y}, g)$*,*

$$d_I(f,g) \le d_{FD}(f,g) \le 3d_I(f,g).$$

4 Relationship Between the Interleaving and Bottleneck Distances

Having strongly equivalent metrics means that we can quickly pass back and forth many of the properties associated to the metrics. For example, the bottleneck stability bound for persistence diagrams in terms of the functional distortion distance [1] says the following (for the definitions of the persistence diagrams $\mathrm{Dg}_0(f), \mathrm{ExDg}_1(f)$ associated to a function f and of the bottleneck distance d_B we refer the reader to [10]):

▶ **Theorem 17** (Bauer, Ge, Wang [1])**.** *Given two Reeb graphs* $(\mathbb{X}, f)$ *and* $(\mathbb{Y}, g)$*,*

$$d_B(\mathrm{Dg}_0(f), \mathrm{Dg}_0(g)) \le d_{FD}(f,g)$$

and

$$d_B(\mathrm{ExDg}_1(f), \mathrm{ExDg}_1(g)) \le 3d_{FD}(f,g).$$

Combining this result with Theorem 16 gives an immediate stability result relating the interleaving distance with the bottleneck distance.

▶ **Corollary 18.** *Given two Reeb graphs* $(\mathbb{X}, f)$ *and* $(\mathbb{Y}, g)$*,*

$$d_B(\mathrm{Dg}_0(f), \mathrm{Dg}_0(g)) \le 3d_I(f,g)$$

and

$$d_B(\mathrm{ExDg}_1(f), \mathrm{ExDg}_1(g)) \le 9d_I(f,g).$$

5 Discussion

In this paper, we study the relationship between two existing distances for Reeb graphs, and show that they are strongly equivalent on the set of Reeb graphs. This relationship will be a powerful tool for understanding convergence properties of the different metrics. For example, if we have a Cauchy sequence in one metric, we have a Cauchy sequence in the other and can therefore pass completeness results back and forth. This relationship also means that algorithms for approximation of the metrics can be written using whichever method is most helpful and applicable to the context.

These two distances may in general not be the same. However, we have yet to find an example for which it can be shown that the two distances are actually different. It is easy to construct examples where the bound $d_I(f,g) \le d_{FD}(f,g)$ of Lemma 8 is tight; the status of the bound $d_{FD}(f,g) \le 3d_I(f,g)$ of Lemma 15 is unclear. While that bound is obtained using an arbitrary selection, a better bound may be achievable using a particular optimal selection. In addition, this may shed light on whether the bounds given between the bottleneck distance of the extended persistence diagrams and the two Reeb graph distances are tight. Finally, we plan to explore the use of these distances for studying the stability of Reeb-like structures, such as Mapper and α-Reeb graphs [24, 4].

References

1 Ulrich Bauer, Xiaoyin Ge, and Yusu Wang. Measuring distance between Reeb graphs. In *Proceedings of the Thirtieth Annual Symposium on Computational Geometry*, SOCG'14, New York, NY, USA, 2014. ACM.

2 Silvia Biasotti, Daniela Giorgi, Michela Spagnuolo, and Bianca Falcidieno. Reeb graphs for shape analysis and applications. *Theoretical Computer Science*, 392(1-3):5–22, February 2008.

3 Kevin Buchin, Maike Buchin, Marc van Kreveld, Bettina Speckmann, and Frank Staals. Trajectory grouping structure. In Frank Dehne, Roberto Solis-Oba, and Jörg-Rüdiger Sack, editors, *Algorithms and Data Structures*, volume 8037 of *Lecture Notes in Computer Science*, pages 219–230. Springer Berlin Heidelberg, 2013.

4 Frédéric Chazal and Jian Sun. Gromov-Hausdorff approximation of filament structure using Reeb-type graph. In *Proceedings of the Thirtieth Annual Symposium on Computational Geometry*, SOCG'14, pages 491:491–491:500, New York, NY, USA, 2014. ACM.

5 Justin Curry. *Sheaves, Cosheaves and Applications.* PhD thesis, University of Pennsylvania, December 2014.

6 Vin de Silva, Elizabeth Munch, and Amit Patel. Categorified Reeb graphs, January 2015.

7 Tamal K. Dey, Fengtao Fan, and Yusu Wang. An efficient computation of handle and tunnel loops via Reeb graphs. *ACM Trans. Graph.*, 32(4):32:1–32:10, July 2013.

8 Barbara Di Fabio and Claudia Landi. The edit distance for Reeb graphs of surfaces, November 2014. `http://arxiv.org/abs/1411.1544`.

9 Harish Doraiswamy and Vijay Natarajan. Output-Sensitive construction of Reeb graphs. *Visualization and Computer Graphics, IEEE Transactions on*, 18(1):146–159, January 2012.

10 Herbert Edelsbrunner and John Harer. *Computational Topology: An Introduction.* Amer. Math. Soc., Providence, Rhode Island, 2010.

11 Francisco Escolano, Edwin R. Hancock, and Silvia Biasotti. Complexity fusion for indexing Reeb digraphs. In Richard Wilson, Edwin Hancock, Adrian Bors, and William Smith, editors, *Computer Analysis of Images and Patterns*, volume 8047 of *Lecture Notes in Computer Science*, pages 120–127. Springer Berlin Heidelberg, 2013.

12 Xiaoyin Ge, Issam I. Safa, Mikhail Belkin, and Yusu Wang. Data skeletonization via Reeb graphs. *Advances in Neural Information Processing Systems*, 24:837–845, 2011.

13 William Harvey, Yusu Wang, and Rephael Wenger. A randomized $O(m \log m)$ time algorithm for computing Reeb graphs of arbitrary simplicial complexes. In *Proceedings of the Twenty Sixth Annual Symposium on Computational Geometry*, SoCG'10, pages 267–276, New York, NY, USA, 2010. ACM.

14 Franck Hétroy and Dominique Attali. Topological quadrangulations of closed triangulated surfaces using the Reeb graph. *Graphical Models*, 65(1-3):131–148, May 2003.

15 Masaki Hilaga, Yoshihisa Shinagawa, Taku Kohmura, and Tosiyasu L. Kunii. Topology matching for fully automatic similarity estimation of 3D shapes. In *Proceedings of the 28th annual conference on Computer graphics and interactive techniques*, SIGGRAPH'01, pages 203–212, New York, NY, USA, 2001. ACM.

16 Ernest Michael. Continuous selections II. *Annals of Mathematics*, 64(3):pp. 562–580, 1956.

17 Dmitriy Morozov, Kenes Beketayev, and Gunther Weber. Interleaving distance between merge trees. Manuscript, 2013.

18 Mattia Natali, Silvia Biasotti, Giuseppe Patanè, and Bianca Falcidieno. Graph-based representations of point clouds. *Graphical Models*, 73(5):151–164, September 2011.

19 Monica Nicolau, Arnold J. Levine, and Gunnar Carlsson. Topology based data analysis identifies a subgroup of breast cancers with a unique mutational profile and excellent survival. *Proceedings of the National Academy of Sciences*, 108(17):7265–7270, 2011.

20 Salman Parsa. A deterministic $O(m \log m)$ time algorithm for the Reeb graph. *Discrete & Computational Geometry*, 49(4):864–878, 2013.

21 Georges Reeb. Sur les points singuliers d'une forme de Pfaff complèment intégrable ou d'une fonction numérique. *Comptes Rendus de L'Académie ses Séances*, 222:847–849, 1946.

22 Dušan Repovš and Pavel V. Semenov. *Continuous Selections of Multivalued Mappings*. Kluwer Academic Publishers, 1998.

23 Yoshihisa Shinagawa, Tosiyasu L. Kunii, and Yannick L. Kergosien. Surface coding based on Morse theory. *IEEE Comput. Graph. Appl.*, 11(5):66–78, September 1991.

24 Gurjeet Singh, Facundo Mémoli, and Gunnar Carlsson. Topological methods for the analysis of high dimensional data sets and 3D object recognition. In *Eurographics Symposium on Point-Based Graphics*, 2007.

25 Zoë Wood, Hugues Hoppe, Mathieu Desbrun, and Peter Schröder. Removing excess topology from isosurfaces. *ACM Transactions on Graphics*, 23(2):190–208, April 2004.

26 Yuan Yao, Jian Sun, Xuhui Huang, Gregory R. Bowman, Gurjeet Singh, Michael Lesnick, Leonidas J. Guibas, Vijay S. Pande, and Gunnar Carlsson. Topological methods for exploring low-density states in biomolecular folding pathways. *The Journal of Chemical Physics*, 130:144115, 2009.